Colloids and Surfaces A: Physicochemical and Engineering Aspects 683 (2024) 132952

Contents lists available at ScienceDirect

Colloids and Surfaces A: Physicochemical and Engineering Aspects

journal homepage: www.elsevier.com/locate/colsurfa

Zeolite A grown on fiberglass: A prominent CO_2 adsorbent for CO_2/CH_4 separation

José D.V. Souza-Filho [a], Edipo S. Oliveira [b], Jadson B. Guedes [b], João B.A. Silva Júnior [c], Conceição R.F. Alves [b], Juliana A. Coelho [d], Ari C.A. Lima [e], Moisés Bastos-Neto [f], José M. Sasaki [g], Francisco S.B. Mota [a], Adonay R. Loiola [b,*]

[a] Department of Civil Engineering, Federal University of Ceará, Fortaleza, CE 60440-900, Brazil
[b] Department of Organic and Inorganic Chemistry, Federal University of Ceará, Fortaleza, CE 60440-900, Brazil
[c] Department of Chemistry, Ceara State University, Tauá, CE 63660-000, Brazil
[d] Faculty of Engineering, Languages and Social Sciences of Seridó, Federal University of Rio Grande do Norte, Currais Novos, RN 59380-000, Brazil
[e] Ceará Industrial Technology Nucleus Foundation, Prof. Rômulo Proença Street, Pici, Fortaleza, CE 60440-552, Brazil
[f] Department of Chemical Engineering, Federal University of Ceará, Fortaleza, CE 60440-900, Brazil
[g] Department of Phisics Federal University of Ceará, Fortaleza, CE 60440-900, Brazil

GRAPHICAL ABSTRACT

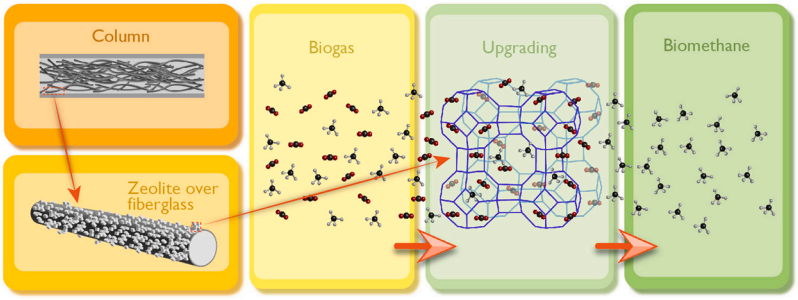

ARTICLE INFO

Keywords:
Zeolite A
Fiberglass
Composite
CO_2 adsorption
CO_2/CH_4 mixture

ABSTRACT

Considerable efforts have been devoted to developing adsorbents capable of retain CO_2 either via direct capture from air, or via more sophisticated systems such as biogas, a mixture from which methane can be upgraded. In this work, we present an experimental investigation of zeolite NaA, grown over alkaline-treated fiberglass, synthesized by means of hydrothermal route and tested as adsorbent for CO_2 removal in the CO_2/CH_4 mixture. Zeolite NaA was successfully obtained, with absence of secondary phases, as detailed by the characterization results. Adsorption experiments, presented in terms of isotherms, demonstrated the potential of the synthesized material as a selective CO_2 adsorbent with potential to be applied for biogas enrichment.

* Corresponding author.
E-mail address: adonay@ufc.br (A.R. Loiola).

https://doi.org/10.1016/j.colsurfa.2023.132952
Received 31 August 2023; Received in revised form 2 December 2023; Accepted 5 December 2023
Available online 7 December 2023

1. Introduction

In the face of the growing demand for renewable energy sources and the environment impacts related to the process of global warming, the development of new technologies for CO_2 capture has become a critical environmental issue, and certainly one of the greatest challenges of the humankind [1]. In this regard, the degradation of urban solid wastes leads to the production of huge amounts biogas, a gaseous mixture composed mainly of methane (CH_4) and carbon dioxide (CO_2), and other minor components such as H_2S, siloxanes, N_2 and water vapor [2]. CH_4 is known to promote harmful impacts on the environment, considering its contribution for the global warming, at least 20 times more aggressively than CO_2 [3]. On the other hand, the CH_4 present in the biogas is a versatile energy source and therefore has a potential to be harnessed and applied in many different fields replacing fossil fuel in electric power generation, vehicle engines, heat production etc.

Nevertheless, the use of biogas as a fuel requires previous treatments aiming the removal of H_2O and H_2S, and the capture of CO_2, a process commonly referred as biogas upgrading [4]. H_2O and H_2S can be removed via relatively simple and low-cost methods, whereas CO_2, in particular for being present in considerable higher concentrations (30–60%), usually demands more robust technologies for its removal. The leading techniques employed for CO_2 removal are physical absorption (washing) [5–7], chemical absorption [8], membrane separation [9] and pressure swing adsorption (PSA) [10]. Other incipient techniques include cryogenic separation [11], in situ enrichment [12], hydrates formation [13], biological methods [14], and carbon mineralization [15]. Among these techniques, PSA stands out given the relatively low costs of operation and the non-generation of residual solvents. The PSA efficiency depends largely on the adsorbent choice, which should be selective towards CO_2, present high adsorption capacity and the ability to undergo regeneration [16,17]. Besides, the adsorbent should be thermally stable, chemically inert, and present high surface area. In this regard, materials such as activated carbons and microporous aluminosilicates [18,19], with emphasis on zeolites [20], have been widely employed in biogas upgrading.

Zeolites are defined as silica-based microporous materials, in which some Si atoms are replaced by other elements as Al (mainly), P, Fe, B, Ga, Ti, Ge etc. Zeolites are characterized by a 3D structure resulting from the bonds between the tetrahedral TO_4 units (T = Si, Al, P, Fe etc.), linked via oxygen atoms. The zeolitic structures present channel and cavity systems with molecular dimensions, capable of reversibly induce the addition and removal of guest compounds, what make them excellent adsorbents [21–23]. Despite all the appealing properties, zeolites possess one important drawback which is associated with their polycrystalline nature, i.e., their powder aspect. For practical applications, zeolites are usually required to be packed as pellets, dramatically reducing the internal available area and therefore their performance. Alternatively, zeolites can be prepared, either associated or not with other materials, in hierarchical structures, in such a way that their crystals are arranged to form interparticle mesopores, or even macropores. Several strategies can be adopted in the preparation of hierarchical zeolites: (i) mesoporosity formed from the controlled degradation of zeolite crystals [24,25], (ii) interparticle mesopores by the arrangement of nanozeolite crystals [26], (iii) zeolite crystallization by using bifunctional surfactants [27–29] and (iv) the crystallization of zeolites over other materials (zeolitization) [30,31], including membranes, a growing field in separation processes [32,33]. Zeolitzation can be accomplished by growth, dispersion, or aggregation of zeolitic crystals over either inorganic or organic materials, leading to formation of bigger pores, to which the zeolite micropores will be connected, as a result of the particles organization. Several different materials have been used as support for zeolite growth, particularly with monolithic features [34–36]. However, materials such as fiber glass can offer certain advantages from mechanical point of view given its malleability.

Herein, we present the preparation of a zeolite composite, with hierarchical features, by coating activated fiberglass with zeolite crystals, grown via hydrothermal route, and the assessment of its performance as CO_2 adsorbent in CO_2/CH_4 mixtures.

2. Experimental

2.1. Zeolite A synthesis

Zeolite A-fiberglass was prepared by using fiberglass, FG, (Synth, 99.5% SiO_2) which underwent an alkaline treatment targeting generation of roughness so that further zeolite nucleation could take place, as reported by Silva et al. [37]. This treatment consisted of immersing 10.0 g of FG in 100.0 mL of NaOH 4.0 mol L^{-1} in a polypropylene flask, and mechanically stirred for 72 h (200 rpm). The activated FG sample (aFG) was then washed with HCl 1.0 mol L^{-1} (2 ×), and with distilled water (2 ×), and finally dried at 80.0 °C for 24 h.

A precursor solution for zeolite synthesis was prepared by dissolving 7.16 g of Na_2SiO_3 (Sigma-Aldrich, 50–53% SiO_2) in 35.0 mL of NaOH 0.21 mol L^{-1} , in a polypropylene beaker, and 5.00 g of $NaAlO_2$ (Sigma-Aldrich, 50–56% of Al_2O_3) with 35.0 mL of NaOH 0.21 mol L^{-1} in another beaker, and then these two solutions were mixed. 8.00 g of the sample aFG was transferred to a Teflon-lined stainless-steel autoclave, together with the precursor solution, reaching the complete volume of the autoclave (72 mL). The system was kept at 25.0 ℃ for 18.0 h and then heated at 100 ℃ for 4 h under autogenous pressure and static conditions. After cooling, the obtained material was washed with distilled water and centrifuged at 4000 rpm (7 ×). To eliminate zeolite crystals which were not formed incorporated onto the fiberglass, water splash was applied to the samples, spread over a sieve as screen protection. This way, it is ensured that the final material is robust to withstand flow either of liquids or gases without having its structure compromised. The sample was named as aFG-Zeo. For comparison purposes, conventional zeolite NaA (Zeolite A) was prepared following the method described by Thompson et al. [38].

2.2. Characterization

X-ray powder diffraction (XRPD) patterns of the samples FG, aFG, aFG-Zeo, and Zeolite A, were obtained by using a Panalytical (X-Pert Pro MPD) x-ray powder diffractometer. The powder patterns were collected in the continuous mode ($\theta - \theta$ scan) with step size of 0.013°(2θ). Monochromatic Co-Kα1 radiation was used, obtained with the tube operating at 40 kV and 40 mA.

Fourier transform infrared (FTIR) spectra of samples in the form of KBr pellets were obtained, at room temperature, on a Shimadzu IRealise FTIR spectrometer in the 4000–400 cm^{-1} region, with a nominal resolution of 2 cm^{-1}.

For scanning electron microscopy (SEM), a Quanta 200 (FEI) microscope was used, by employing detector for secondary electrons and energy-dispersed X-ray. Samples were dispersed over a conductive carbon double-sided sticky tape, on aluminum supports. To reduce charging effects, the samples were coated with a thin layer of gold (ca. 20 nm).

CO_2 adsorption isotherms were obtained at 273 K in an Autosorb-iQ$_3$ equipment (Quantachrome, USA) and used to characterize the micropore volume of the studied zeolites. The samples (ca. 0.1 g) were previously degassed under the following conditions: heating under high vacuum (10^{-4} mbar), from room temperature to 180 ℃, at a heating rate of 2 ℃ min^{-1} , maintaining at the final temperature for a period of 6 h. The microporous volume was calculated using the Dubinin-Radushkevich equation.

2.3. Adsorption experiments

Isotherms of pure CH_4, pure CO_2, and a 47% CH_4/53% CO_2 (v/v) were obtained at 25 ℃ up to 10 bar using a magnetic suspension balance

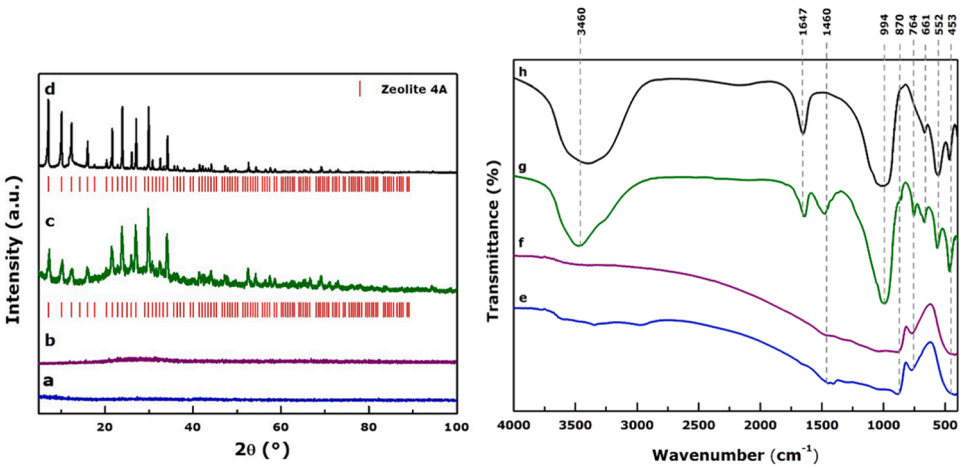

Fig. 1. Co-Kα XRD patterns for the samples (a) FG, (b) aFG, (c) aFG-Zeo, and (d) powder zeolite A. FTIR, in KBr, for the samples (e) FG, (f) aFG, (g) aFG-Zeo, and (h) powder zeolite A.

Rubotherm (Bochum, Germany), equipped with a mixture unit. Before the equilibrium essays, the samples (ca. 0.5 g) were thermally treated at 300 ℃ with heating rate of 2 ℃ min^{-1} , under vacuum, for 10 h.

The adsorption isotherms data were fitted to Langmuir and Sips isotherm models, Eqs. 1 and 2.

$$q_{Lang} = \frac{q_{\max} bP}{1 + bP} \tag{1}$$

$$q_{Sips} = \frac{q_{\max} (bP)^n}{1 + (bP)^n} \tag{2}$$

Where q is the amount adsorbed at a partial pressure P, q_{max} is the maximum amount that could be adsorbed, b is the parameter of affinity between adsorbate and adsorbent and n is a parameter of Sips model that characterize the heterogeneity of the system.

The CO_2/CH_4 selectivity was calculated using the Eq. 3, which q_{CO2} and q_{CH4} were obtained from Langmuir and Sips models.

$$\alpha_{CO2/CH4} = \frac{q_{CO2}/y_{CO2}}{q_{CH4}/y_{CH4}} \tag{3}$$

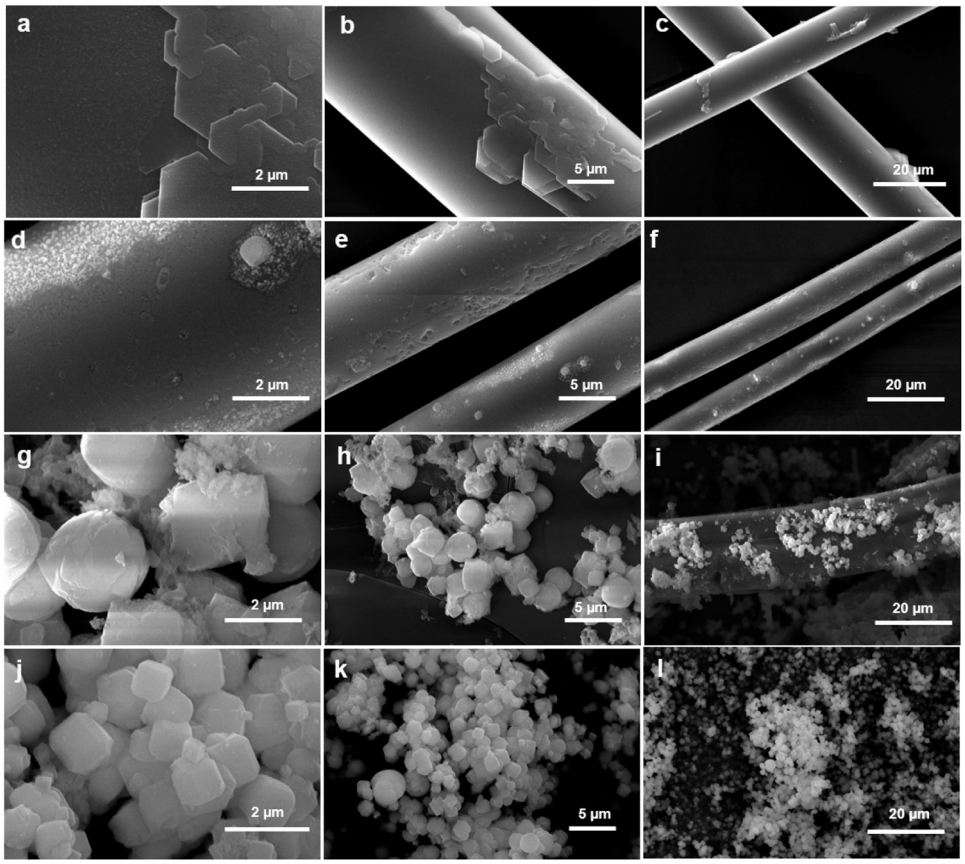

Fig. 2. SEM images of samples (a-c) FG, (d-f) aFG, (g-i) aFG-Zeo, and (j-l) zeolite NaA.

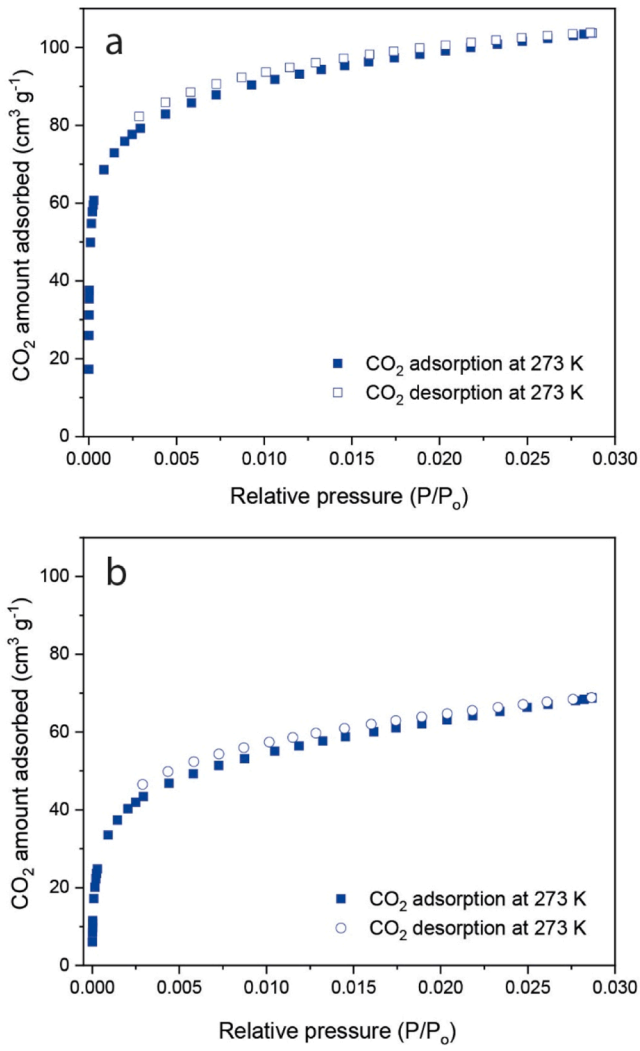

Fig. 3. Standard experimental isotherms of CO_2 (273 K) of (a) zeolite A and (b) glass fiber-zeolite A.

3. Results and discussion

3.1. Characterization

XRPD patterns of the prepared samples are shown in Fig. 1, together with the FTIR spectra. The fiberglass, sample FG (Fig. 1a), underwent alkaline treatment aiming a surface partial deformation so that some homogeneous roughness could be generated, facilitating the nucleation of zeolite crystals in the subsequent synthesis stage. The XRD pattern of the alkaline activated sample, aFG, (Fig. 1b) indicates that no structural change occurred, with its amorphous nature been preserved. The intense diffraction peaks observed in Fig. 1c are consistent with zeolite A (ICSD 24901), indicating its crystallization, without other signals which could be associated with secondary phases. When the relative intensity of the peaks referent to the samples aFG-Zeo and Zeolite A are compared, it is observed that the first three peaks of the samples aFG-Zeo, with 2θ equal to 7.203°, 10.193°, and 12.492° (Fig. 1c) are less intense. Such characteristic is associated with a specific amount of zeolite A crystals generated over the fiberglass surface. The reduction in intensity of the peaks of a crystalline material on a glass surface has been observed in other studies involving fiberglass and is consistent with the zeolite synthesis over such material [39]. The observed background is result of the core fiberglass over which the zeolite crystals were formed.

FTIR provides invaluable information related to the structure of the

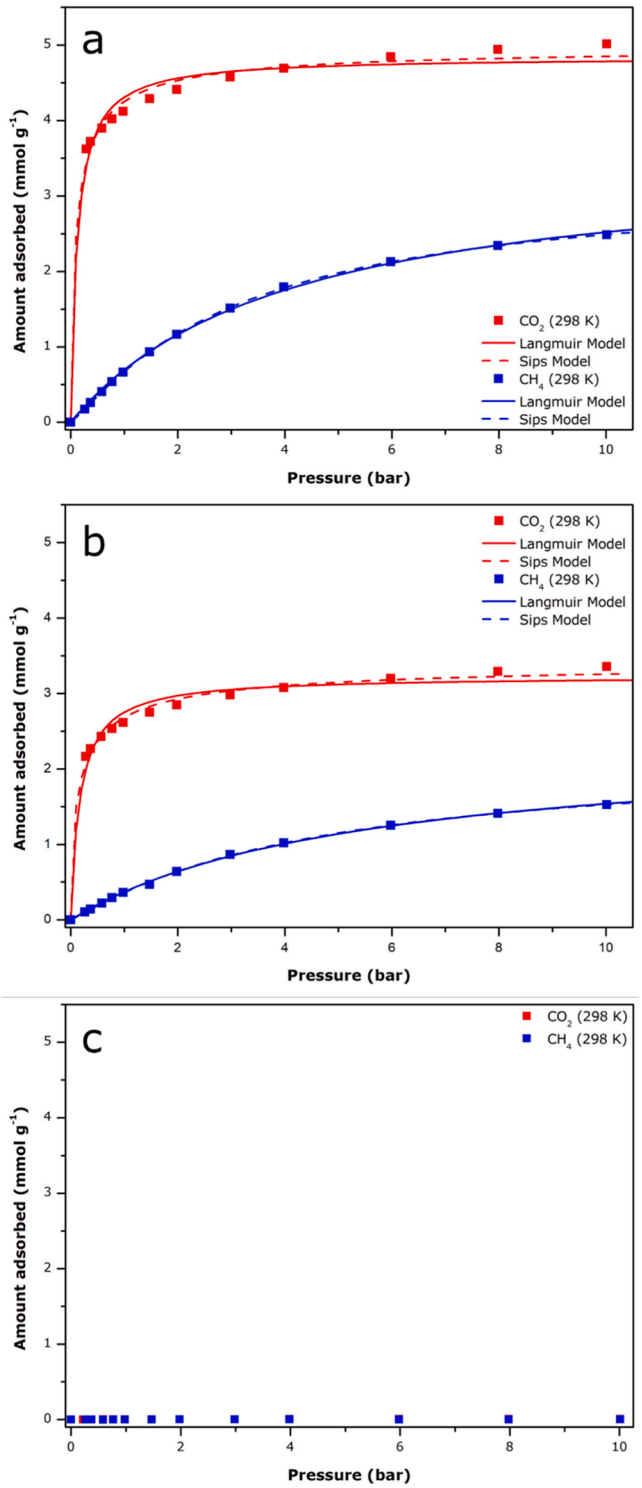

Fig. 4. Adsorption isotherms of CO_2 and CH_4 at 298 K for the samples (a) zeolite A, (b) aFG-Zeo, and (c) aFG. Langmuir and Sips equilibrium models were applied to the experimental data.

synthesized zeolite and can therefore be useful as a complementary tool for XRD data interpretation. The FTIR spectrum of zeolite A, presented in Fig. 1h, shows characteristic bands of the zeolite. The intense signal centered at 994 cm^{-1} is consistent with Si(Al)–O asymmetric stretching [40]. The three signals below 990 cm^{-1} are part of what is known as the fingerprint region. The band at 661 cm^{-1} is associated with internal vibration of the (Si, Al)–O symmetric stretching. The band observed at 552 cm^{-1} is related to the external vibration of the double four-rings

Table 1
Fitting parameters of Langmuir model and Sips model.

Langmuir	q_m (mmol g^{-1})		b (bar^{-1})		n		R^2	
	CO_2	CH_4	CO_2	CH_4			CO_2	CH_4
Zeolite A	4.84	3.55	8.09	0.24	-		0.99307	0.99963
aFG-Zeo	3.23	2.37	5.76	0.19	-		0.99126	0.99961
Sips	q_m (mmol g^{-1})		b (bar^{-1})		n		R^2	
	CO_2	CH_4	CO_2	CH_4	CO_2	CH_4	CO_2	CH_4
Zeolite A	4.99	3.19	9.73	0.31	0.77	1.12	0.99629	0.99998
aFG-Zeo	3.46	2.17	6.44	0.22	0.67	1.07	0.99732	0.99974

structure, which connects the β-cage, and the band at 453 cm^{-1} corresponds to internal vibration of (Si, Al)–O bending [41]. The presence of structural water is confirmed by the large band at 3460 cm^{-1} [41,42]. All these bands are also observed in the spectrum of the sample aFG-Zeo, the zeolite grown over the fiberglass (Fig. 1i), accompanied by the bands at 764 cm^{-1} , and 870 cm^{-1} and 1460 cm^{-1} . These later are also present in the spectrum of the sample aFG and are related to the fiber structure.

SEM images of all the samples are presented in Fig. 2. The sample FG (Fig. 2a-c) is composed of fibers with surface predominantly smooth, with uniform texture, which gives rise to a rough surface, but still in a controlled way, when submitted to alkaline treatment (Fig. 2d-f). The formation of zeolite crystals over the surface of the alkaline activated fiberglass sample is easily observable in Fig. 2g-i. The zeolite A typical crystals with cubic habit are formed directly over the activated fiberglass, with prevalence in regions of the fiberglass surface where the roughness is more evident. To emphasize the zeolite synthesis efficiency in presence of the fiberglass, zeolite A crystals, in the powder form, are shown in Fig. 2j-l, allowing direct comparison. The loading amount of zeolite over the fiberglass surface was estimated in 45–50%, based on the X-ray fluorescence analysis combined with the evaluation of a series of SEM images of the treated fiberglass, the pure zeolite, and fiberglass covered with the zeolite.

Textural properties such as surface area, pore volume and pore size distribution are essential to understand the porous structures of zeolitic materials. N_2 (at 77 K) and Ar (at 87 K) are the two most common gases used as probe. Nevertheless, their rate of diffusion at low temperature into zeolite A micropores limits their application in this sense [43]. Alternatively, CO_2 has been applied as a useful strategy for such cases, with isotherms obtained at 273 K, even though some characteristics related to the strong CO_2–CO_2 interaction and the incipient theoretical background still possess some challenges for its effective application [42,44]. CO_2 adsorption isotherms for zeolite A and aFG-Zeo samples are presented in Fig. 3.

The specific micropore volume of zeolite A and aFG-Zeo samples calculated from CO_2 adsorption isotherms at 273 K are 0.23 cm^3g^{-1} and 0.17 cm^3g^{-1}, respectively. This reduction on the specific micropore volume occurs because the fiberglass does not contribute to the microporosity of the samples.

3.2. Adsorption isotherms

The isotherms of pure CH_4 and CO_2, obtained for the samples of zeolite A, aFG-Zeo, and aFG are presented in Fig. 4. As expected, zeolite A presented high affinity for CO_2 at low pressures, as indicated by the rectangular shape of CO_2 isotherm (Fig. 4a), with adsorption capacity comparable to those verified in previous works [45,46]. The higher affinity towards CO_2 compared to CH_4 results from its higher critical temperature, i.e., CO_2 presents a condensable vapor behavior in the given conditions and is therefore less volatile than CH_4, and so easier adsorbed [47]. The CO_2 adsorption capacity, at 10 bar and 298 K, decreases from ca. 5 mmol g^{-1} , in sample zeolite A, to ca. 3 mmol g^{-1} in sample aFG-Zeo (Fig. 4b), which can be seen as a satisfactory result considering that the later contains less zeolite. The fiberglass, over which the zeolite crystals are dispersed, does not contribute to CO_2 adsorption, as shown in Fig. 4c.

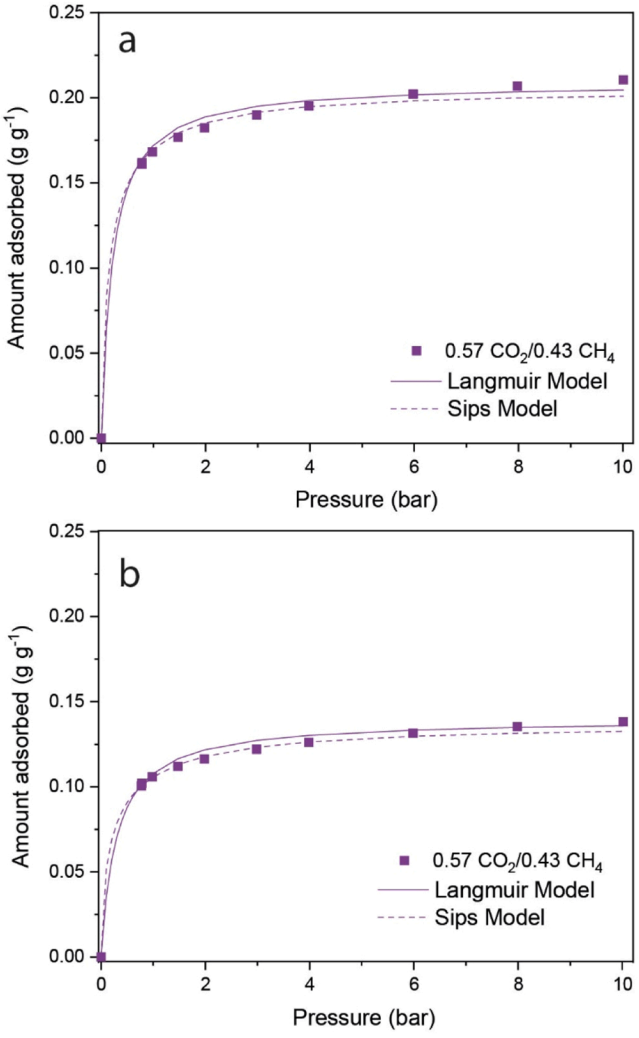

Fig. 5. Adsorption biogas upgrading experiment with mixture 57% CO_2/43% CH_4 for samples (a) zeolite A and (b) aFG-Zeo.

The fitting parameters of Langmuir model and Sips model for CO_2 and CH_4 adsorption isotherms on zeolite A and aFG-Zeo are presented in Table 1. Both models fit satisfactorily the experimental data, showing $R^2 > 0.99$, although the Sips model showed better fitting. The presence of fiberglass reduces the value of all parameters. The decrease in q_{max} value occurs because de fiberglass does not contribute to CO_2 and CH_4 on the studied conditions.

The isotherms of the mixture of 43% CH_4/57% CO_2 (v/v) are shown in Fig. 5, together with the prediction of the extended models of Langmuir and Sips (Eqs. 4 and 5, respectively). As expected, both models fitting satisfactorily the experimental data for mixtures of CH_4 and CO_2, showing $R^2 > 0.99$.

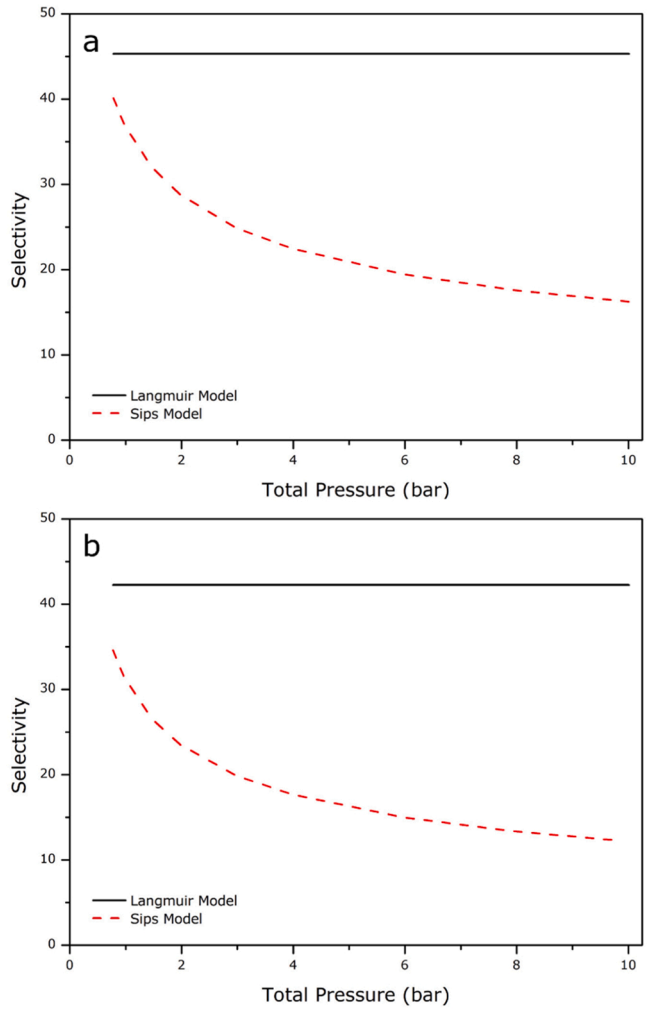

Fig. 6. CO_2/CH_4 selectivity calculated using Langmuir model and Sips model for samples (a) zeolite A and (b) aFG-Zeo.

$$q_{i,Lang} = \frac{q_{\max,i} b_i P_i}{1 + \sum_{j=1}^{N} b_j P_j} \tag{4}$$

$$q_{i,Sips} = \frac{q_{\max,i} (b_i P_i)^n}{1 + \sum_{j=1}^{N} (b_j P_j)^n} \tag{5}$$

The selectivity of CO_2/CH_4 (Fig. 6) was calculated using the predict amount adsorbed of each gas by Lagmuir model and Sips model. The Langmuir model gives a constant selectivity correspondent to the ratio between the affinity parameter of CO_2 and CH_4 for each sample, while the Sips model give a decreasing selectivity that varies between 40 and 16 for zeolite A, and 35 and 12 for aFG-Zeo sample. These results show that the fiberglass over which the zeolite crystals are grown reduce the selectivity less than 35%, which can be seen as acceptable considering its structural role, i.e., to support the zeolite crystals.

4. Conclusion

Zeolite NaA was successfully synthesized over alkaline-activated fiberglass surface by employing a simple and low-cost strategy, with absence of secondary crystalline phases. The hydrothermal treatment applied to the fiberglass allowed a surface modification that resulted in controlled roughness, a condition that facilitated the growth of zeolite crystals. Adsorption essays showed that the obtained material presented appreciable CO_2 adsorption capacity as well as high selectivity towards CO_2 in CO_2/CH_4 mixtures, attesting its potential for biogas upgrading, with the differential approach of being a non-powder material, easily to be handled and more effective regarding diffusional barriers.

Ackownledgments

This study was financed in part by the Coordenação de Aperfeiçoamento de Pessoal de Nível Superior - Brasil (CAPES) - CAPES/PROEX: 23038.000509/2020-82 and CNPq (Proces: 402561/2007-4) Call MCT/CNPq n.10-2007 for the XRD analyses. The authors would also to thank the Central Analítica-UFC/CT-Infra/MCTI/SISNANO/Pró-Equipamentos CAPES for the technical support on SEM analyses.

CRediT authorship contribution statement

Coelho Juliana A.: Data curation, Investigation, Methodology, Writing – original draft. **Silva Júnior João B. A.:** Formal analysis, Investigation, Methodology. **Alves Conceição R. F.:** Data curation, Investigation, Methodology. **Oliveira Edipo S.:** Conceptualization, Formal analysis, Investigation, Methodology, Writing – original draft, Writing – review & editing. **Guedes Jadson B.:** Formal analysis, Investigation, Methodology. **Loiola Adonay:** Conceptualization, Data curation, Formal analysis, Funding acquisition, Project administration, Supervision, Writing – original draft, Writing – review & editing. **Souza-Filho José D. V.:** Conceptualization, Formal analysis, Investigation, Methodology, Writing – original draft. **Sasaki José M.:** Conceptualization, Investigation, Supervision, Writing – original draft. **Mota Francisco S. B.:** Data curation, Investigation, Methodology, Resources, Writing – original draft. **Lima Ari C. A.:** Formal analysis, Investigation, Methodology. **Bastos-Neto Moisés:** Formal analysis, Investigation, Methodology, Writing – original draft, Writing – review & editing.

Declaration of Competing Interest

The authors declare that they have no known competing financial interests or personal relationships that could have appeared to influence the work reported in this paper.

Data Availability

Data will be made available on request.

References

[1] M. Bui, C.S. Adjiman, A. Bardow, E.J. Anthony, A. Boston, S. Brown, P.S. Fennell, S. Fuss, A. Galindo, L.A. Hackett, J.P. Hallett, H.J. Herzog, G. Jackson, J. Kemper, S. Krevor, G.C. Maitland, M. Matuszewski, I.S. Metcalfe, C. Petit, G. Puxty, J. Reimer, D.M. Reiner, E.S. Rubin, S.A. Scott, N. Shah, B. Smit, J.P.M. Trusler, P. Webley, J. Wilcox, N. Mac, Dowell, Carbon capture and storage (CCS): the way forward, Energy Environ. Sci. 11 (2018) 1062–1176.
[2] H.G. Katariya, H.P. Patolia, Advances in biogas cleaning, enrichment, and utilization technologies: a way forward, Biomass Conversion and Biorefinery, (2021).
[3] M. Ritzkowski, R. Stegmann, Controlling greenhouse gas emissions through landfill in situ aeration, Int. J. Greenh. Gas. Control 1 (2007) 281–288.
[4] R. Kadam, N.L. Panwar, Recent advancement in biogas enrichment and its applications, Renew. Sustain. Energy Rev. 73 (2017) 892–903.
[5] F. Wang, G. Kang, D. Liu, M. Li, Y. Cao, Enhancing CO_2 absorption efficiency using a novel PTFE hollow fiber membrane contactor at elevated pressure, AIChE J. 64 (2018) 2135–2145.
[6] R. Noorain, T. Kindaichi, N. Ozaki, Y. Aoi, A. Ohashi, Biogas purification performance of new water scrubber packed with sponge carriers, J. Clean. Prod. 214 (2019) 103–111.
[7] C. Ma, C. Liu, X. Lu, X. Ji, Evaluation and comparison of aqueous ChCl/Urea and other physical absorbents for biogas upgrading process, Energy Procedia 142 (2017) 3631–3636.
[8] S. Singhal, S. Agarwal, S. Arora, P. Sharma, N. Singhal, Upgrading techniques for transformation of biogas to bio-CNG: a review, Int. J. Energy Res. 41 (2017) 1657–1669.

[9] F.M. Baena-Moreno, M. Rodríguez-Galán, F. Vega, L.F. Vilches, B. Navarrete, Review: recent advances in biogas purifying technologies, Int. J. Green. Energy 16 (2019) 401–412.
[10] R.L.S. Canevesi, K.A. Andreassen, E.A. da Silva, C.E. Borba, C.A. Grande, Pressure swing adsorption for biogas upgrading with carbon molecular sieve, Ind. Eng. Chem. Res. 57 (2018) 8057–8067.
[11] Y. Tan, W. Nookuea, H. Li, E. Thorin, J. Yan, Cryogenic technology for biogas upgrading combined with carbon capture - a review of systems and property impacts, Energy Procedia 142 (2017) 3741–3746.
[12] N. Aryal, T. Kvist, F. Ammam, D. Pant, L.D.M. Ottosen, An overview of microbial biogas enrichment, Bioresour. Technol. 264 (2018) 359–369.
[13] B. Castellani, F. Rossi, M. Filipponi, A. Nicolini, Hydrate-based removal of carbon dioxide and hydrogen sulphide from biogas mixtures: experimental investigation and energy evaluations, Biomass Bioenergy 70 (2014) 330–338.
[14] B. Tao, A.M. Alessi, Y. Zhang, J.P.J. Chong, S. Heaven, C.J. Banks, Simultaneous biomethanisation of endogenous and imported CO_2 in organically loaded anaerobic digesters, Appl. Energy 247 (2019) 670–681.
[15] K. Starr, X. Gabarrell, G. Villalba, L. Talens, L. Lombardi, Life cycle assessment of biogas upgrading technologies, Waste Manag. 32 (2012) 991–999.
[16] H.J. Choi, J.G. Min, S.H. Ahn, J. Shin, S.B. Hong, S. Radhakrishnan, C.V. Chandran, R.G. Bell, E. Breynaert, C.E.A. Kirschhock, Framework flexibility-driven CO_2 adsorption on a zeolite, Mater. Horiz. 7 (2020) 1528–1532.
[17] G. Singh, J. Lee, A. Karakoti, R. Bahadur, J. Yi, D. Zhao, K. AlBahily, A. Vinu, Emerging trends in porous materials for CO_2 capture and conversion, Chem. Soc. Rev. 49 (2020) 4360–4404.
[18] O. Cheung, Z. Bacsik, Q. Liu, A. Mace, N. Hedin, Adsorption kinetics for CO_2 on highly selective zeolites NaKA and nano-NaKA, Appl. Energy 112 (2013) 1326–1336.
[19] H.A. Patel, J. Byun, C.T. Yavuz, Carbon dioxide capture adsorbents: chemistry and methods, ChemSusChem 10 (2017) 1303–1317.
[20] Y.Y. Jiang, J.H. Ling, P. Xiao, Y.D.A. He, Q.H. Zhao, Z. Chu, Y.S. Liu, Z.Y. Li, P. A. Webley, Simultaneous biogas purification and CO_2 capture by vacuum swing adsorption using zeolite NaUSY, Chem. Eng. J. 334 (2018) 2593–2602.
[21] M. Moliner, C. Martínez, A. Corma, Multipore Zeolites: Synthesis and Catalytic Applications, Angew. Chem. Int. Ed. 54 (2015) 3560–3579.
[22] R.M. Barrer, Zeolites and their synthesis, Zeolites 1 (1981) 130–140.
[23] C.G. Li, M. Moliner, A. Corma, Building zeolites from precrystallized units: nanoscale architecture, Angew. Chem. -Int. Ed. 57 (2018) 15330–15353.
[24] A. Corma, From microporous to mesoporous molecular sieve materials ans their use in catalysis, Chem. Rev. 97 (1997) 2373–2419.
[25] D.P. Serrano, J.M. Escola, P. Pizarro, Synthesis strategies in the search for hierarchical zeolites, Chem. Soc. Rev. 42 (2013) 4004–4035.
[26] W. Schwieger, A.G. Machoke, T. Weissenberger, A. Inayat, T. Selvam, M. Klumpp, A. Inayat, Hierarchy concepts: classification and preparation strategies for zeolite containing materials with hierarchical porosity, Chem. Soc. Rev. 45 (2016) 3353–3376.
[27] K. Na, C. Jo, J. Kim, K. Cho, J. Jung, Y. Seo, R.J. Messinger, B.F. Chmelka, R. Ryoo, Directing Zeolite Structures into Hierarchically Nanoporous Architectures, Science 333 (2011) 328–332.
[28] M. Choi, K. Na, J. Kim, Y. Sakamoto, O. Terasaki, R. Ryoo, Stable single-unit-cell nanosheets of zeolite MFI as active and long-lived catalysts, Nature 461 (2009) 246–U120.
[29] Y.J. Zhang, P. Luo, H. Xu, L. Han, P. Wu, H. Sun, S.N. Che, Hierarchical MFI zeolites with a single-crystalline sponge-like mesostructure, Chem. -A Eur. J. 24 (2018) 19300–19308.
[30] P. Losch, M. Boltz, K. Soukup, I.H. Song, H.S. Yun, B. Louis, Binderless zeolite coatings on macroporous α-SiC foams, Microporous Mesoporous Mater. 188 (2014) 99–107.
[31] M.W. Anderson, S.M. Holmes, N. Hanif, C.S. Cundy, Hierarchical pore structures through diatom zeolitization, Angew. Chem. -Int. Ed. 39 (2000) 2707–2710.
[32] W. Huang, Z. He, B. Liu, Q. Wang, S. Zhong, R. Zhou, W. Xing, Large surface-to-volume-ratio and ultrahigh selectivity SSZ-13 membranes on 61-channel monoliths for efficient separation of CO_2/CH4 mixture, Sep. Purif. Technol. 311 (2023), 123285.
[33] N. Wang, G. Dang, Z. Bai, Q. Wang, B. Liu, R. Zhou, W. Xing, In situ synthesis of cation-free zirconia-supported zeolite CHA membranes for efficient CO_2/CH4 separation, ACS Appl. Mater. Interfaces 15 (2023) 16853–16864.
[34] A. Huang, F. Liang, F. Steinbach, J. Caro, Preparation and separation properties of LTA membranes by using 3-aminopropyltriethoxysilane as covalent linker, J. Membr. Sci. 350 (2010) 5–9.
[35] Z. Wang, Q. Ge, J. Shao, Y. Yan, High performance zeolite LTA pervaporation membranes on ceramic hollow fibers by dipcoating−wiping seed deposition, J. Am. Chem. Soc. 131 (2009) 6910–6911.
[36] X. Yang, Y. Liu, C. Yan, G. Chen, Solvent-free preparation of hierarchical 4A zeolite monoliths: Role of experimental conditions, J. Cryst. Growth 528 (2019), 125286.
[37] E.S. Oliveira, C.R.F. Alves, A.M.M. França, R.F. Nascimento, J.M. Sasaki, A. R. Loiola, NaA zeolite synthesized over finerglass as a strategy for optimizing hard water softening, Quím. Nova 45 (2022) 16–22.
[38] R.W. Thompson, M.J. Huber, Analysis of the growth of molecular sieve zeolite NaA in a batch precipitation system, J. Cryst. Growth 56 (1982) 711–722.
[39] K. Okada, K. Kuboyama, T. Takei, Y. Kameshima, A. Yasumori, M. Yoshimura, In situ zeolite Na-X coating on glass fibers by soft solution process, Microporous Mesoporous Mater. 37 (2000) 99–105.
[40] Y. Huang, Z. Jiang, Vibrational spectra of completely siliceous zeolite A, Microporous Mater. 12 (1997) 341–345.
[41] A.R. Loiola, J.C.R.A. Andrade, J.M. Sasaki, L.R.D. da Silva, Structural analysis of zeolite NaA synthesized by a cost-effective hydrothermal method using kaolin and its use as water softener, J. Colloid Interface Sci. 367 (2012) 34–39.
[42] B.C. Amoni, A.D.L. Freitas, R.A. Bessa, C.P. Oliveira, M. Bastos-Neto, D.C. S. Azevedo, S.M.P. Lucena, J.M. Sasaki, J.B. Soares, S.A. Soares, A.R. Loiola, Effect of coal fly ash treatments on synthesis of high-quality zeolite A as a potential additive for warm mix asphalt, Mater. Chem. Phys. 275 (2022), 125197.
[43] F. Rouquerol, J. Rouquerol, K. Sing, CHAPTER 11 - Adsorption by Clays, Pillared Layer Structures and Zeolites, in: F. Rouquerol, J. Rouquerol, K. Sing (Eds.), Adsorption by Powders and Porous Solids, Academic Press, London, 1999, pp. 355–399.
[44] S.M.P. Lucena, J.C.A. Oliveira, D.V. Gonçalves, L.M.O. Lucas, P.A.S. Moura, R. G. Santiago, D.C.S. Azevedo, M. Bastos-Neto, LTA zeolite characterization based on pore type distribution, Ind. Eng. Chem. Res. 61 (2022) 2268–2279.
[45] P.A.S. Moura, D.P. Bezerra, E. Vilarrasa-Garcia, M. Bastos-Neto, D.C.S. Azevedo, Adsorption equilibria of CO_2 and CH_4 in cation-exchanged zeolites 13X, Adsorp. J. Int. Adsorp. Soc. 22 (2016) 71–80.
[46] H. Golipour, B. Mokhtarani, M. Mafi, A. Moradi, H.R. Godini, Experimental measurement for adsorption of ethylene and ethane gases on copper-exchanged zeolites 13X and 5A, J. Chem. Eng. Data 65 (2020) 3920–3932.
[47] M. Tagliabue, D. Farrusseng, S. Valencia, S. Aguado, U. Ravon, C. Rizzo, A. Corma, C. Mirodatos, Natural gas treating by selective adsorption: material science and chemical engineering interplay, Chem. Eng. J. 155 (2009) 553–566.